

R. PASCHOTTA

Noise of mode-locked lasers (Part II): timing jitter and other fluctuations

Ultrafast Laser Physics, Institute of Quantum Electronics, Swiss Federal Institute of Technology,
ETH Hönggerberg HPT, 8093 Zürich, Switzerland

Received: 19 February 2004/Revised version: 22 April 2004
Published online: 31 May 2004 • © Springer-Verlag 2004

ABSTRACT This work presents a comprehensive discussion of the noise properties of mode-locked lasers, with an emphasis on the effect of quantum noise in passively mode-locked solid-state lasers. Of special interest is the timing jitter, which is coupled to noise in various other pulse parameters. The study is based on analytical results and on numerical tools as described in part one of this study. It results in useful guidelines for the comparison and optimization of different kinds of lasers concerning timing jitter.

PACS 43.50.+y, 42.50.Lc, 42.60.Fc

1 Introduction

In part one of this article [1], I have described in detail a numerical model which can simulate the evolution of noise in the pulses circulating in a mode-locked laser and calculate the corresponding noise spectra. Here I present a comprehensive study of a wide range of noise phenomena in mode-locked lasers. New analytical results show that earlier results from the Haus/Mecozzi model [2], which is based on soliton perturbation theory, are valid in a much wider range of situations, including cases without any soliton effects. On the other hand, it becomes apparent that additional aspects of interest, such as passive mode locking with a slow saturable absorber, can not easily be covered with extensions of the Haus/Mecozzi model. Also, a realistic description of the generation of intensity noise and its influence on timing noise are difficult, although ref. [3] presents a significant step in this direction. As shown in this article, additional analytical results can be derived to describe the coupling from intensity to timing noise through various effects. The numerical model then serves to test the analytical results, not only by checking against trivial errors but also to test whether other phenomena of importance have been overlooked. Furthermore, the numerical model is required for more complicated cases which are not fully accessible by analytical techniques.

Basic limitations for the achievable noise levels in mode-locked lasers arise from quantum effects. It is important to

point out that there are two different kinds of such limitations. First, there are fundamental limits to the noise properties of pulses, which apply to any pulsed source which does not exhibit squeezing effects. Besides the well-known shot noise limit for the intensity noise, there is a fundamental limit for the timing jitter, as discussed in Sect. 2. Second, there are limitations of the noise properties of mode-locked lasers which arise from quantum effects acting in these lasers. These limitations are discussed in Sects. 3 to 7. The resulting low-frequency timing noise on the output of mode-locked lasers is often orders of magnitude above the mentioned fundamental quantum limit, even in cases where quantum noise is the dominating noise source in the laser cavity. In short, the laser dynamics transform internal quantum noise inputs into noise on the output pulses which is far above the quantum limit. Therefore, it can be confusing to talk about quantum-limited noise performance when it is not clear which type of limitation is meant. Note also that the mentioned excess noise can be easily reduced with feedback loops, while these would not allow getting below the basic quantum limit, at least not outside the feedback loop.

For laser development and applications, it is important to understand the relations between various design parameters and the expected noise performance. The discussion in Sects. 3 to 7 shows that a large part of these relations is in fact easy to understand. Therefore, a set of simple design guidelines are obtained which will allow optimization of the noise performance of lasers without performing detailed simulations in each case. Also, these guidelines allow a general comparison of different types of lasers in Sect. 8.

The analytical and numerical tools used here are also very useful for a study of noise in the optical phase and in the carrier-envelope offset. These issues, which are relevant in a somewhat different context, will be treated elsewhere.

For a detailed description of the notation and some mathematical background, see Sect. 2 in part one of this article [1].

2 Quantum noise limits for amplitude noise and timing jitter

In the following section, it is assumed that no squeezing effects occur, i.e., that the variances in both quadrature components of the optical amplitudes are equal. It is well known that this causes so-called shot noise in the intensity, and this noise also occurs in pulse trains. There is probably

less awareness that the same quantum noise also leads to a certain timing jitter of a pulse train.

For the following analysis a semiclassical description of quantum noise is always used. At the quantum limit of a non-squeezed beam, there are complex amplitude fluctuations with Gaussian probability distributions and an autocorrelation given by:

$$G_{\delta A}(\tau) \equiv \langle \delta A^*(t) \delta A(t + \tau) \rangle = \frac{h\nu}{2} \delta(\tau), \quad (1)$$

where the amplitude is normalized so that its squared modulus is the optical power, and $h\nu$ is the photon energy. For light with a constant average power \bar{P} , the autocorrelation of the corresponding intensity noise is

$$G_{\delta P}(\tau) \equiv \langle \delta P(t) \delta P(t + \tau) \rangle = \bar{P} h\nu \delta(\tau). \quad (2)$$

If this is applied to a single pulse in a pulse train, it is found that the variance of the photon number equals the average photon number:

$$\left(\frac{1}{h\nu} \right)^2 \sigma_{\delta E_p}^2 = \frac{\langle E_p \rangle}{h\nu}. \quad (3)$$

This corresponds to the well-known shot noise with a two-sided power density

$$S_{\delta P}(f) = P_{av} h\nu, \quad (4)$$

of the intensity noise, and to the one-sided spectral power density

$$L(f) = \frac{2}{P_{av}^2} S_{\delta P}(f) = \frac{2 h\nu}{P_{av}}, \quad (5)$$

of the relative intensity noise for the average power P_{av} of the pulse train.

Now consider the timing noise. The pulse has an optical power $P(t) = \bar{P}(t) + \delta P(t)$ where $\bar{P}(t)$ corresponds to a noiseless pulse shape, e.g. of sech^2 -shaped form, centered at $t = 0$. The superimposed noise somewhat shifts the pulse position, although on average this shift is zero. The variance of the pulse position is

$$\begin{aligned} \sigma_{t_m}^2 &= \frac{1}{E_p^2} \left\langle \left(\int t \delta P(t) dt \right)^2 \right\rangle \\ &= \frac{1}{E_p^2} \left\langle \int \int t t' \delta P(t) \delta P(t') dt dt' \right\rangle \\ &= \frac{1}{E_p^2} \left\langle \int \int t t' (A^*(t) \delta A(t) + \text{c.c.}) \right. \\ &\quad \left. \times (A^*(t') \delta A(t') + \text{c.c.}) dt dt' \right\rangle \\ &= \frac{1}{E_p^2} \int \int t t' \left(2\bar{P}(t) \frac{h\nu}{2} \delta(t-t') \right) dt dt' \\ &= \frac{h\nu}{E_p^2} \int t^2 \bar{P}(t) dt. \end{aligned} \quad (6)$$

For example, for a sech^2 -shaped pulse with full width at half maximum (FWHM) duration τ_p , this gives

$$\begin{aligned} \sigma_{t_m}^2 &= \frac{h\nu}{E_p^2} \int t^2 P(t) dt = \frac{\pi^2}{12 (2\text{arcosh}\sqrt{2})^2} \frac{h\nu}{E_p} \tau_p^2 \\ &\approx 0.2647 \frac{h\nu}{E_p} \tau_p^2, \end{aligned} \quad (7)$$

while for a Gaussian pulse the constant factor would be ≈ 0.1803 instead of 0.2647.

For a quantum-limited pulse train with repetition rate f_{rep} , the timing errors of different pulses are uncorrelated, and results in a white noise with a two-sided spectral power density

$$S_{t_m}(f) = \frac{\sigma_{t_m}^2}{f_{\text{rep}}} \approx 0.2647 \frac{h\nu}{P_{av}} \tau_p^2 \quad (8)$$

for sech^2 -shaped pulses. This means that within a measurement bandwidth B the variance is

$$\sigma_{t_m}^2 = S_{t_m} 2B \approx 0.2647 \frac{h\nu}{P_{av}} \tau_p^2 2B \quad (9)$$

(with $2B$ instead of B , because a two-sided power density is used). For example, consider a 1064-nm pulse train with 100 mW average output power, $\tau_p = 1$ ps, $B = 1$ MHz: $\sigma_{t_m}^2 \approx (1 \text{ as})^2$.

This fundamental limit is really rather low, and its detection in an experiment would be demanding. As explained in the introduction, it is important not to confuse this limit with the level of timing jitter produced by a mode-locked laser which is subject only to unavoidable quantum noise inputs. At low noise frequencies, such lasers typically exhibit a timing noise far above the fundamental limit. The following sections, however, show that all mode-locked lasers should reach the fundamental limit at high noise frequencies.

Note that at the quantum limit for the timing jitter the timing noise power is proportional to the square of the pulse duration. This means that the noise power of the timing jitter relative to the average pulse duration is constant. Also, it is possible to calculate the recorded noise power on a photodiode, caused by the timing noise at the quantum limit, in the form of the one-sided normalized spectral power density:

$$L(f) \approx S_{\varphi}(f) \approx 0.2647 (2\pi f_{\text{rep}} \tau_p)^2 \frac{h\nu}{P_{av}}. \quad (10)$$

By comparing this with (5), it can be seen that this noise stays below the shot noise level in many cases, where $f_{\text{rep}} \tau_p \ll 1$. However, some multi-GHz picosecond lasers [4, 5] are not operating in this regime. Also, even if the phase noise contribution to a photodiode signal would disappear below the shot noise, more refined measurement schemes, which can be based on an optical phase detector method [6], should still be able to detect this phase noise.

3 Timing noise in simple cases with a fast saturable absorber

3.1 Effect of quantum noise

3.1.1 Intracavity pulses. In the simplest case, a passively mode-locked laser has no intracavity dispersion and no non-linearity. Mode locking is achieved with a fast saturable absorber, and influence from pump noise is neglected.

Although this situation is not identical to the one in Sect. 2, it is possible to build on those results. First, only the intracavity pulse is considered. During each round-trip, it is subject to spontaneous emission noise from the gain medium and to additional quantum noise associated with losses. Neglecting the variation of gain within the pulse spectrum, it was found that the gain and (wavelength-independent) loss contribute equal amounts of noise. In total, the added complex noise amplitudes have the autocorrelation

$$G_{\delta A}(\tau) \equiv \langle \delta A^*(t) \delta A(t + \tau) \rangle = h\nu g \delta(\tau). \quad (11)$$

(Note that in this article g is the intensity gain, not the amplitude gain as in [2].)

In analogy to the calculation in Sect. 2, this yields

$$\Delta\sigma_{t_m}^2 = \frac{h\nu}{E_p^2} 2g \int t^2 \bar{P}(t) dt \quad (12)$$

per cavity round-trip to the timing variance, so that the variance is growing with time according to

$$\sigma_{\Delta t}^2(t) \equiv \langle (t_m(t) - t_m(0))^2 \rangle = \frac{h\nu}{E_p^2} 2g \left(\int t'^2 \bar{P}(t') dt' \right) \frac{t}{T_{rt}}. \quad (13)$$

The linear dependence on the time shows that this describes a random walk. The corresponding spectral power density is proportional to f^{-2} , and the constant factor can be obtained by inserting the ansatz $S_{\Delta t}(f) = C f^{-2}$ into the calculation of the temporal variance:

$$\begin{aligned} \sigma_{\Delta t}^2(t) &\equiv \langle (t_m(t) - t_m(0))^2 \rangle = 2 (G_{t_m}(0) - G_{t_m}(t)) \\ &= 8 \int_0^{+\infty} S_{\Delta t}(f) \sin^2(\pi f T) df \end{aligned} \quad (14)$$

The result is

$$S_{\Delta t}(f) = \frac{1}{(2\pi f)^2} \frac{h\nu}{E_p^2} \frac{2g}{T_{rt}} \int t^2 P(t) dt, \quad (15)$$

which evaluates to

$$S_{\Delta t}(f) \approx 0.5294 \frac{1}{(2\pi f)^2} \frac{h\nu}{E_p} \frac{g}{T_{rt}} \tau_p^2 \quad (16)$$

for sech²-shaped pulses. This is exactly one half of the original result of [2], eq. (69) taking only the second term, which corresponds to the direct influence of quantum noise on the timing jitter. After correcting the trivial errors in the diffusion

constants, as shown in part one of this paper, perfect agreement with the new result is obtained.

The new result is significant because it explains why the equation can be applied to cases without soliton pulses. The basic mechanism of the temporal shift, adding spontaneous emission noise to the pulse in each cavity round-trip, is in no way related to the mechanism which forms the average pulse shape. Thus, the restricting assumptions of [2], which are clearly not fulfilled in this simple case without solitons, are actually not necessary for the result. Of course, the timing noise will have additional contributions in more complicated cases. However, the obtained noise term is unavoidable as long as there is no mechanism which can provide a restoring force for the pulse position which depends on the current timing error. Such a restoring force occurs in actively mode-locked lasers, which therefore behave differently, but not in free-running passively mode-locked lasers.

The result can also be easily generalized to lasers with other pulse shapes, simply using modified values for the term $\int t^2 \bar{P}(t) dt$.

Note that the fast saturable absorber has no influence on the timing jitter, apart from somewhat increasing the required gain. This is because even a strong saturable absorber cannot provide a restoring force for the pulse position.

3.1.2 Output pulses. One might expect that the timing jitter of the output pulses is the same as the jitter of the intracavity pulses. However, as already mentioned in part one, the output pulses are also influenced by zero-point fluctuations of the vacuum field reflected at the output coupler mirror. This effect is well known in quantum optics [7] and sets a minimum noise level which is reached for high noise frequencies. In fact this noise level is at the fundamental quantum limit (see Sect. 2).

Note that the power density of the timing noise of the intracavity pulses scales with f^{-2} , so that it goes below the fundamental quantum limit at high noise frequencies. This fact may seem surprising, but it has a simple explanation: for low cavity losses in particular, the pulses circulate in the cavity without much noise being added. Therefore, the change of the temporal position within a few round-trips can be very small, so that the noise is highly correlated over short times. This corresponds to a low high-frequency noise, potentially below the standard quantum limit. However, these noise properties of the internal pulses can not be directly observed, and for the output pulses the quantum limit applies due to the reflected vacuum fluctuations.

3.1.3 Dependence on laser parameters. Note that the noise power from (15) is proportional not only to the gain or to the cavity loss, but also to $1/T_{rt}$, simply because this determines how often per second the noise from the gain medium and from the losses acts on the pulse. One can also interpret the dependence of the noise power on g/T_{rt} as a dependence on the cold cavity bandwidth [8] (i.e., the cavity bandwidth with the gain switched off), which happens to be also proportional to g/T_{rt} , although the arguments given above appear to lead to the more elucidating physical interpretation.

The timing jitter of a mode-locked laser can be reduced by making its cavity longer, because this lets the gain medium

and the losses disturb the pulse position less frequently. However, a longer cavity can also lead to increased timing noise if it leads to greatly increased fluctuations of the cavity length (see Sect. 3.2) due to a less stable mechanical setup.

The timing noise power is also inversely proportional to the intracavity pulse energy, except for the output pulses at high noise frequencies, where the noise level is set by the output pulse energy. These dependencies are not surprising, as quantum fluctuations always have a lower impact at higher power levels, where the photon number per pulse is larger.

3.2 Effect of mirror vibrations

Here the influence of fluctuations of the optical cavity length on the timing jitter is considered. Such fluctuations can occur as a result of vibrations of intracavity mirrors, but can also arise from refractive index fluctuations (due to thermal effects) in the gain medium, for example.

Assume first a sinusoidal oscillation of the round-trip time with the small amplitude δT_{rt} and the frequency f , starting at $t = 0$. In a passively mode-locked laser, this will cause an accumulated timing error (for $t > 0$) of

$$\Delta t(t) = \frac{1}{T_{\text{rt}}} \int_0^t \delta T_{\text{rt}} \sin 2\pi f t' dt' = -\frac{1}{T_{\text{rt}}} \delta T_{\text{rt}} \frac{\cos 2\pi f t}{2\pi f} \quad (17)$$

(where an arbitrary oscillation phase has been omitted), which is oscillating with an amplitude $\frac{1}{2\pi f T_{\text{rt}}} \delta T_{\text{rt}}$. It is important to realize that the timing error is related to the change of round-trip time via an integration, which causes a $1/f$ dependence. Also there is the dependence on $1/T_{\text{rt}}$, because the timing error is increased more often per second when T_{rt} is small.

The result can be generalized for an arbitrary spectral power density $S_{T_{\text{rt}}}(f)$ of the fluctuations of the round-trip time. This causes a contribution

$$\Delta S_{\Delta t}(f) = \left(\frac{1}{2\pi f T_{\text{rt}}} \right)^2 S_{T_{\text{rt}}}(f) \quad (18)$$

to the timing noise, to be added to the power density of the (uncorrelated) timing noise from other sources.

For example, if there is a simple mechanical resonance of a mirror mount, this will lead to $S_{T_{\text{rt}}}(f) \propto f^{-2}$ far above the resonance frequency, if the vibrations are excited by a white noise source. This leads to a timing noise contribution with $\Delta S_{\Delta t}(f) \propto f^{-4}$. Therefore, it is conceivable that the 20-dB discrepancy between the measured timing jitter and the calculated jitter based on quantum noise as reported in [2] might not be due to errors in the experimental parameters but rather to the fact that mirror vibrations are the actual limitation for jitter in this Ti:sapphire laser.

Note that for actively mode-locked lasers, the effect of changes of the round-trip time is much more complicated, because here the modulator introduces a restoring force for the timing error. This does not simply reduce the timing error, but rather leads to complicated dynamics, possibly including complicated instabilities with strongly increased timing jitter, if the modulator frequency is not precisely matched to the natural round-trip frequency. Such phenomena have been discussed in [9].

4 Center frequency fluctuations

In Sect. 3 it was found that spontaneous emission noise in the gain medium can have a direct effect on the timing jitter, leading to $S_{\Delta t}(f) \propto f^{-2}$. Another, more indirect channel, has been pointed out by Haus and Mecozzi [2]: spontaneous emission also causes fluctuations of the center frequency of the pulse, which can couple to the timing noise through the intracavity dispersion.

As in the case of the direct effect of quantum noise on the timing jitter, this mechanism works in the same way for a much broader class of lasers, where soliton effects do not necessarily dominate over other pulse shaping effects. In fact, in the following I show a derivation which does not at all depend on soliton perturbation theory.

In this case, amplitudes (envelopes) $A(f)$ in the frequency domain (see part one), are normalized so that $\int_{-\infty}^{+\infty} |A(f)|^2 df$ is the pulse energy. Taking a noiseless pulse spectrum and considering its temporal shift per round-trip which is associated with adding a noise amplitude with the autocorrelation gives

$$G_{\delta A}(\Delta f) \equiv \langle \delta A^*(f) \delta A(f + \Delta f) \rangle = h\nu g \delta(\Delta f). \quad (19)$$

The center frequency is

$$f_c = f_{\text{ref}} + \frac{\int f |A(f)|^2 df}{\int |A(f)|^2 df} = f_{\text{ref}} + \frac{1}{E_p} \int f |A(f)|^2 df, \quad (20)$$

and the increase of its variance per round-trip, caused by spontaneous emission, is

$$\begin{aligned} \Delta \sigma_{f_c}^2 &= \frac{1}{E_p^2} \left\langle \left(\int f (A^*(f) \delta A(f) + \text{c.c.}) df \right)^2 \right\rangle \\ &= \frac{h\nu}{E_p^2} 2g \int f^2 |A(f)|^2 df \end{aligned} \quad (21)$$

by analogy to (12). So by ignoring the fact that the limited gain spectrum will pull the pulse spectrum back towards f_{ref} , a variance increasing linearly with time is obtained, that is consistent with a spectral power density of

$$S_{f_c}(f) = \frac{1}{(2\pi f)^2} \frac{h\nu}{E_p^2} 2g \int f'^2 |A(f')|^2 df'. \quad (22)$$

The restoring force caused by the finite gain spectrum can now be included, which effectively inserts a high pass filter and modifies the result to

$$S_{f_c}(f) = \frac{1}{(2\pi f)^2 + \tau_f^{-2}} \frac{h\nu}{E_p^2} 2g \int f'^2 |A(f')|^2 df', \quad (23)$$

as in [2], with

$$\tau_f = \frac{3T_{\text{rt}} (\pi \Delta f_g)^2 (\tau_p/1.763)^2}{2g} \quad (24)$$

for sech²-shaped pulses. In that case, there is also

$$\frac{1}{E_p} \int f^2 |A(f)|^2 df \approx 0.2647 \Delta f_p^2 \quad (25)$$

where $\Delta f_p \approx 0.315/\tau_p$ is the soliton bandwidth. The result turns out to be exactly consistent with the one of the Haus/Mecozzi model [2], using the corrected diffusion constant D_p of the erratum [10] (or 33 in part one).

The mechanism which transfers noise in the center frequency to timing noise is as described in [2]. If the center frequency is offset by a value Δf_c , the total intracavity dispersion D_2 per round-trip (corresponding to $2D$ in [2]) translates this into a timing error $D_2 (2\pi \Delta f_c)$ per round-trip. The total timing noise spectrum is then

$$S_{\Delta t}(f) = \frac{1}{(2\pi f)^2} \frac{h\nu}{E_p^2} 2 \frac{g}{T_{rt}} \int t^2 P(t) dt + \left(\frac{D_2}{f T_{rt}} \right)^2 S_{f_c}(f), \quad (26)$$

where the first term shows the direct effect of spontaneous emission and the second term the dispersion-mediated effect. This equation is consistent with (69) in [2] (with corrected diffusion constants).

In conclusion, it can be seen that the Haus/Mecozzi result ((69) in [2]) is valid not only in cases where soliton perturbation theory can be applied. Also, the result for other than sech^2 -shaped pulse spectra can be easily generalised, where the power density changes by a constant factor.

In order to minimize the contribution of the fluctuating center frequency to the timing jitter, one may minimize the dispersion. In a soliton mode-locked laser, this also requires minimizing the Kerr nonlinearity, and this optimization will eventually be limited by the required crystal length or by the need to maintain strong enough soliton shaping effects. For most picosecond lasers, the zero-dispersion point is ideal anyway for minimizing the chirp of the pulses. Note that for longer pulses the first term in (26) tends to become larger, while the second term tends to become smaller due to the small pulse bandwidth, so that minimization of the dispersion may then not be required.

For any case, the low-frequency part of the center frequency noise can be at least minimized by using the gain medium with the smallest gain bandwidth which still supports pulses with the desired duration, or by inserting a bandwidth-limiting filter into the cavity [11].

5 Intensity noise

Before considering the timing noise of mode-locked lasers with additional features, the intensity noise is discussed, which can also couple to the timing noise, as discussed in Sect. 6.

A prerequisite for obtaining realistic intensity noise spectra is to implement a realistic model for gain saturation. In the Haus/Mecozzi model [2], the saturation dynamics are described with the simple assumption that the gain depends only on the instantaneous pulse energy, but not on its history. Particularly for solid-state lasers, this is not a valid assumption, because the saturation energy of the solid-state gain medium is typically orders of magnitude higher than the intracavity pulse energy. Therefore, the gain saturates only through the combined effect of many pulses, leading to phenomena such as relaxation oscillations which do not occur in the simple model of [2]. This calls for the gain (or the inversion density to be used) as an additional dynamical variable, as discussed

in part one. Although an analytical extension in this direction has been described [3], full flexibility is only achieved with a numerical model as the one described in part one.

A first simulation was done without pump noise. Figure 1 shows the intensity noise spectrum of the intracavity pulses (black points) and of the output pulses (gray points). The parameters are the same as in Fig. 2 of part one, except that a realistic gain model with an upper-state lifetime of $20 \mu\text{s}$ has been assumed. One clearly sees the relaxation oscillation peak at the expected position (251 kHz calculated from the parameters). The output pulses approach the shot-noise level at high frequencies, while the intracavity pulses go below the shot noise level for reasons similar to those discussed in Sect. 3.1.2.

In the next simulation, excess noise of the pump, 40 dB above the shot noise level, is included, as it may occur for pumping with a high power diode bar. As Fig. 2 shows, this raises the low-frequency noise more than the noise at the relaxation oscillation frequency, so that the relaxation oscillation peak is now less pronounced on the logarithmic scale.

The observed behavior is similar to the behavior of continuous-wave lasers, as discussed in [12]. However, there is an important difference: due to the action of the sat-

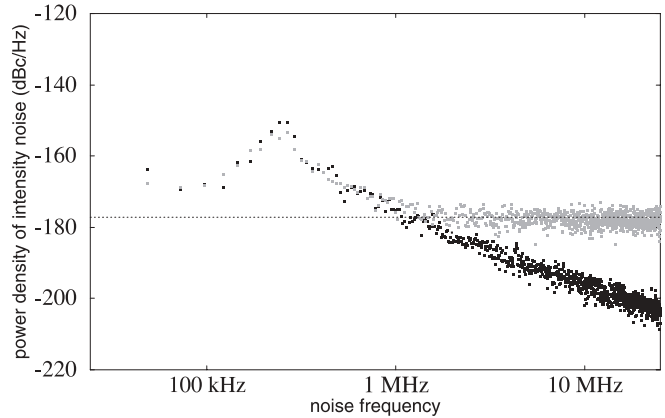


FIGURE 1 Spectrum of relative intensity noise of a laser without dispersion and Kerr nonlinearity, where the parameters are the same as in Fig. 2 of part one of this paper, except for an upper-state lifetime of $20 \mu\text{s}$. Black points: noise of the intracavity pulses. Gray points: noise of the output pulses, reaching the shot-noise level at high frequencies, which is indicated as a dashed line. The vertical axis displays $10 \lg(S_I(f) \times 1 \text{ Hz})$

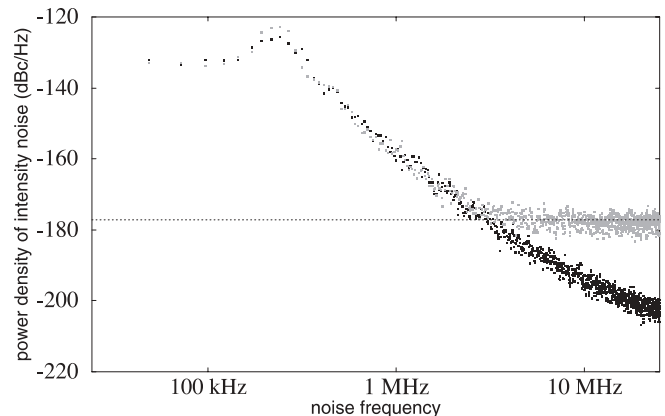


FIGURE 2 Same as Fig. 1, but with pump noise 40 dB above the shot noise level

urable absorber, the damping of the relaxation oscillations is reduced, so that the relaxation oscillation peak becomes higher and more narrow. If the absorber action is sufficiently strong, the laser can even get into the Q-switched mode-locked regime, where the pulse energy undergoes undamped oscillations. This regime has been investigated mostly for slow saturable absorbers [13, 14], but qualitatively it is similar for fast absorbers. Recently, the relaxation oscillations in the stable regime have been investigated for slow saturable absorbers [15].

6 Coupling between intensity noise and timing noise

In the Haus/Mecozzi model [2], (69) for the timing noise does not show an influence of intensity noise. However, these calculations started with a term for Kramers–Krönig-related phase changes in the master equation, which was later dropped without notice. This term would couple the timing noise to fluctuations of the gain, which themselves would be associated with intensity fluctuations.

In the following I discuss several mechanisms providing a coupling from intensity noise to timing jitter.

6.1 Slow saturable absorber

It is known that a pulse is temporally shifted by the action of a slow saturable absorber, because the leading part is attenuated more than the trailing part. While one might think that this shift only causes a slight reduction of the pulse repetition rate, equivalent to a very small increase of the cavity length, the shift actually has at least two important consequences.

The first consequence has been discussed in [16]: it allows stable operation even with absorber recovery times which can be more than 10 times longer than the pulse duration, despite the existence of a time window with net gain behind the pulse, in which one would normally expect any noise to grow without bounds, thus destabilizing the circulating pulse. However, the temporal shift caused by the absorber limits the number of round-trips in which this noise can be amplified, so that stability can be achieved.

As the magnitude of the shift depends on the pulse energy, this is a mechanism which can translate intensity noise into

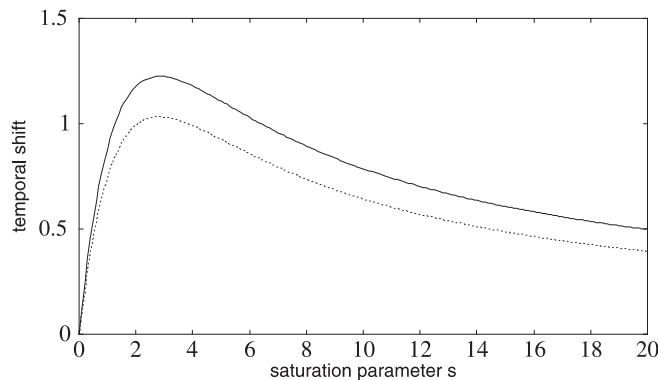


FIGURE 3 Temporal shift of a pulse, caused by a saturable absorber with 1% modulation depth, plotted versus the saturation parameter, in units of $1/1000$ of the pulse duration. The solid line is for sech^2 -shaped pulses, and the dotted line for Gaussian pulses

timing noise, which is another important consequence of the temporal shift caused by the absorber. For asymmetric pulse shapes, a similar effect could occur with fast absorbers. In the following, the focus is on slow saturable absorbers in order to obtain results which are useful for application to lasers which are passively mode-locked with semiconductor saturable absorber mirrors (SESAMs) [17, 18].

The temporal shift is proportional to the modulation depth (maximum reflectivity change) of the absorber and to the pulse duration [16]. Figure 3 shows the magnitude of the shift for 1% modulation depth as a function of the so-called saturation parameter s , which is the ratio of intracavity pulse energy and saturation energy of the absorber.

For small fluctuations, the given function can be linearized around the average value of s , and shows that the timing deviation Δt caused by the intensity noise evolves according to

$$\frac{\partial}{\partial t} \Delta t = \frac{1}{T_{\text{rt}}} \frac{\partial \Delta t}{\partial s} \Delta s = \frac{1}{T_{\text{rt}}} \frac{\partial \Delta t}{\partial s} s \Delta I \quad (27)$$

where ΔI is the relative change of intensity (or pulse energy). For the spectral power densities this results in the relation

$$\Delta S_{\Delta t}(f) = \left(\frac{1}{2\pi f T_{\text{rt}}} \frac{\partial \Delta t}{\partial s} s \right)^2 S_I(f) \quad (28)$$

in analogy to (18), and for the timing phase noise this yields

$$\begin{aligned} \Delta S_{\varphi}(f) &= (2\pi f_{\text{rep}})^2 \Delta S_{\Delta t}(f) = \left(\frac{f_{\text{rep}}}{f T_{\text{rt}}} \frac{\partial \Delta t}{\partial s} s \right)^2 S_I(f) \\ &= \left(\frac{f_{\text{rep}}^2}{f} \frac{\partial \Delta t}{\partial s} s \right)^2 S_I(f), \end{aligned} \quad (29)$$

where the latter equation holds only for lasers with a single pulse in the cavity, so that $f_{\text{rep}} = 1/T_{\text{rt}}$.

Equation 29 reveals an interesting phenomenon. By operating the slow absorber with the value of s for which the maximum temporal shift occurs (i.e., with $s \approx 2.9$ for sech^2 -shaped pulses, see Fig. 3), $\frac{\partial \Delta t}{\partial s} = 0$ can be achieved, and thus the coupling from intensity to timing noise can be eliminated, while higher or lower values of s would lead to some coupling. Fortunately, such a value of s is realistic, it is close to the value where the pulse duration is minimized [16] in the situation without dispersion and nonlinearity, and this moderate saturation level avoids problems with absorber damage. Only in cases where Q-switching instabilities [14] are difficult to suppress, one may be forced to operate the absorber with a higher value of s . Note also that although the saturation behavior or the pulse shape may in reality somewhat differ from the assumptions made in the model, there always exists a value of s where the coupling vanishes.

In order to test (29), a comparison of the spectra of relative intensity noise and timing noise in a numerical simulation can be done. Assuming the same situation as in Fig. 2, also with a pump noise 40 dB above the quantum noise level, except that a slow absorber with the same modulation depth (0.5%) and $s = 5$ is used instead of the fast absorber, the timing noise spectrum shown in Fig. 4 can be obtained. This shows an increase of the timing phase noise at the relaxation oscillation frequency by ≈ 11 dB to -229 dBc/Hz. Comparing this with

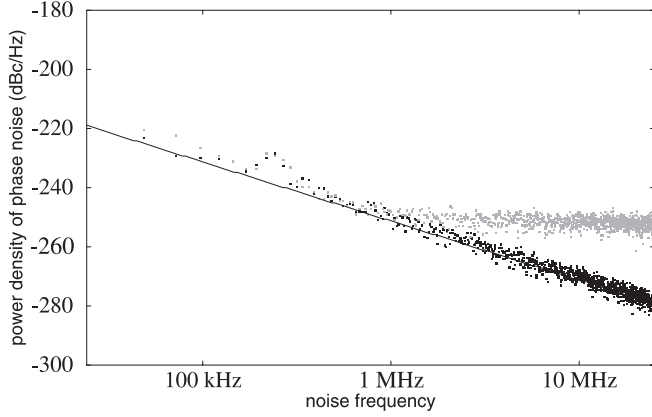


FIGURE 4 Timing phase noise for a laser similar to the one in Fig. 2, but with a slow saturable absorber and saturation parameter $s = 5$. The solid line indicates the analytical result for the intracavity pulses without intensity/timing coupling. As always, the vertical axis displays $10 \log (S_\varphi(f) \times 1 \text{ Hz})$ in dBc/Hz, rather than directly $S_\varphi(f)$ in rad^2/Hz

the peak height in the spectrum of the relative intensity noise (not shown, but similar to Fig. 2), gives a 107-dB difference, while the corresponding difference as expected from (29) would be 106 dB, in reasonable agreement with the numerical result. Other simulations with a lower saturation parameter of $s = 3$ showed that there is no increase of timing noise in this case, as expected given the strongly reduced value of $\frac{\partial \Delta t}{\partial s}$.

Note that near the threshold for Q-switched mode locking (which is reached by reducing the pump power), the relaxation oscillation peak and thus the timing jitter become much stronger.

Inspection of the coupling factor in (29) indicates in which regimes there is a strong coupling from intensity to timing noise. Particularly for lasers with a single circulating pulse (where $f_{\text{rep}} = 1/T_{\text{rt}}$), this is the case when the repetition rate is high; the power density of the timing phase noise caused by amplitude noise grows in proportion to f_{rep}^5 if $S_I(f) \propto f_{\text{rep}}$, while the contribution from other sources usually grows only in proportion to f_{rep}^3 . Also there is stronger coupling for lower noise frequencies, because the timing noise is an integrated effect of changes in the round-trip time (see (17)).

6.2 Kramers–Krönig-related phase changes

As already discussed in Sect. 2.3 in part one of this article, the phase changes associated with a spectrally limited optical gain may provide only a small contribution to the cavity dispersion but may nevertheless have a significant impact on the timing jitter. This is because these phase changes can cause a group delay for the pulse, and this group delay depends on the inversion level, the noise of which can be caused by pump fluctuations and is coupled to intensity noise.

While a numerical model can easily handle phase changes associated with an arbitrary spectral gain profile, it can be helpful to consider the effect of a simple Lorentzian gain line with a peak intensity gain g_p and a FWHM gain bandwidth $\Delta\nu_g$:

$$g(\nu) = \frac{g_p}{1 + \left(2 \frac{\nu - \nu_0}{\Delta\nu_g}\right)^2}. \quad (30)$$

This corresponds to a phase profile

$$\varphi(\nu) = kL n(\nu) = g_p \frac{(\nu - \nu_0) / \Delta\nu_g}{1 + \left(2 \frac{\nu - \nu_0}{\Delta\nu_g}\right)^2} \quad (31)$$

and to a group index according to

$$n_g(\omega) = n(\omega) + \omega \frac{\partial n(\omega)}{\partial \omega}, \quad (32)$$

which leads to a maximum additional group delay

$$T_g(\nu_0) = \frac{g_p}{2\pi \Delta\nu_g} \quad (33)$$

at the line center. This relation shows how changes in the gain translate into changes in the group delay and thus the timing of the pulses. Note that such a link exists even in the center of the symmetric gain line, although the phase change vanishes at this point. The group delay depends on the spectral slope of this phase change, which is non-zero. For arbitrary gain shapes or for amplification away from the gain center, the relation between gain and group delay is modified, and in general there is also a gain-dependent phase change, which can be described by Henry's linewidth enhancement factor α [19]. The coupling to the timing jitter is then determined by the spectral slope $\partial\alpha/\partial\nu$ of the linewidth enhancement factor.

The contribution to the timing jitter for the simple case of a Lorentzian gain line can now be estimated. Fluctuations of the gain translate into changes of the timing according to

$$T_{\text{rt}} \frac{\partial}{\partial t} \Delta t = \frac{\delta g}{2\pi \Delta f_g}, \quad (34)$$

which leads to the following contribution to the timing noise:

$$\Delta S_{\Delta t}(f) = \left(\frac{1}{4\pi^2 f T_{\text{rt}} \Delta f_g} \right)^2 S_g(f). \quad (35)$$

It is now of interest to relate the gain fluctuations to the intensity fluctuations, which are more easily measured. If it is first assumed that the cavity losses are constant (which is actually not strictly true in passively mode-locked lasers), then it is found that a sinusoidal oscillation of the gain with amplitude δg and frequency f causes a pulse energy oscillation with amplitude $\delta E_p = \frac{E_p}{2\pi f T_{\text{rt}}} \delta g$ (where E_p is the average pulse energy). (The derivation is similar as for the results of Sect. 3.2.) Generalizing for arbitrary noise spectra yields

$$S_I(f) = \left(\frac{1}{2\pi f T_{\text{rt}}} \right)^2 S_g(f) \quad (36)$$

for the spectrum of the relative intensity noise. Combined with (35) this leads to

$$\Delta S_{\Delta t}(f) = \left(\frac{1}{2\pi \Delta f_g} \right)^2 S_I(f), \quad (37)$$

or for the timing phase noise to

$$\Delta S_\varphi(f) = (2\pi f_{\text{rep}})^2 \Delta S_{\Delta t}(f) = \left(\frac{f_{\text{rep}}}{\Delta f_g} \right)^2 S_I(f). \quad (38)$$

It is remarkable that the coupling factor depends only on the gain bandwidth but not on the parameters governing gain saturation, nor on the noise frequency. The strongest impact on the timing jitter is expected around the relaxation oscillation frequency. Particularly for solid-state lasers with long upper-state lifetime, the intensity noise in this region can be strong. Note, however, that even a weaker intensity noise peak at higher frequencies can be more important for the timing jitter, as the latter tends to have lower other contributions at higher frequencies. Also note that the influence of gain fluctuations on the timing is the strongest for gain media with narrow linewidth, which are used in lasers for relatively long pulses.

In passively mode-locked lasers, fluctuations of the pulse energy also affect the cavity losses. The Fourier components of the fluctuations of pulse energy E_p , gain g , and saturable loss q (averaged over one pulse), are related to each other by

$$\delta E_p(\omega) = \frac{E_p}{i\omega T_{rt}} (\delta g(\omega) - \delta q(\omega)), \quad (39)$$

where $\delta q(\omega) \approx \frac{\partial q}{\partial E_p} \delta E_p(\omega)$ is the effective loss modulation, assuming full absorber recovery in one round-trip time and small fluctuations. At low noise frequencies, this leads to $\delta g(\omega) \approx \delta q(\omega)$ and thus to the relation

$$S_g(f) \approx \left| \frac{\partial q}{\partial E_p} E_p \right|^2 S_I(f) \quad (40)$$

instead of (36), and the general result for all noise frequencies is

$$S_g(f) = \left[(2\pi f T_{rt})^2 + \left(E_p \frac{\partial q}{\partial E_p} \right)^2 \right] S_I(f), \quad (41)$$

so that with (35) it can be shown that

$$\Delta S_{\Delta t}(f) = \left(\frac{1}{2\pi \Delta f_g} \right)^2 \left[1 + \left(\frac{1}{2\pi f T_{rt}} E_p \frac{\partial q}{\partial E_p} \right)^2 \right] S_I(f) \quad (42)$$

instead of (37).

Finally, the cavity losses and/or the effective gain may fluctuate due to external influences such as vibrations of cavity mirrors which are associated with misalignment of the cavity. This would lead to additional noise of gain and timing.

For a numerical test, I have used the parameters of the last section, with a slow absorber and $s = 2.9$, so that there is no intensity/timing coupling at the absorber. In addition, the Kramers–Krönig phase changes in the gain medium are included (section 3.3.1 in see part one). This indeed leads to a peak in the timing phase noise spectrum at the relaxation oscillation frequency. The height of this peak is in good agreement with the value calculated from (42) and the simulated intensity noise.

Note that the Haus/Mecozzi model [2] originally used a term $\Delta a = -\frac{g}{\Omega_g} \frac{\partial}{\partial t} a$ in the master equation, which is consistent with (33). This term, however, was dropped later on without notice and did not appear in the result for the timing jitter. In any case, the gain fluctuations in a solid-state laser

would not be correctly described by the simple gain saturation model used in this work. However, the extended model of [3] could be used.

6.3 Kerr nonlinearity with self-steepening effect

It is well known that the nonlinear polarization induced in the gain medium causes an intensity-dependent optical phase shift in proportion to the laser intensity. Very often, an approximation is used which results only in this phase shift, but no group delay. As already discussed in part one, section 2.3, one can avoid this approximation in the propagation equation by inserting the so-called self-steepening term [20].

Without any dispersion, one can show that the change of the group velocity for the peak of the pulse is three times larger than the change of phase velocity. Here, however, the pulse shape is increasingly deformed, the peak is delayed more than the wings, so that the trailing slope becomes steeper and steeper. (This effect motivated the name self-steepening.) In the presence of dispersion, however, the overall pulse shape can be preserved, and the reduction of group velocity results from an average effect on the whole pulse. For soliton pulses one can show [21] that the effective group index change for the whole pulse is twice the change of the refractive index for the peak. For other pulse shapes, for higher-order dispersion, or for discrete amounts of dispersion and nonlinearity in the cavity, these effects can be somewhat modified. In any case, one must be aware of a possible effect on the timing jitter.

For an analytical estimate, consider the change of timing caused by the self-steepening effect in one cavity round-trip for a soliton mode-locked laser. The temporal shift of the pulse is two optical cycles per 2π nonlinear peak phase shift $\varphi_{nl} = \gamma P_p$:

$$\Delta t = 2 \frac{\varphi_{nl}}{2\pi} \frac{1}{v_0}. \quad (43)$$

For the spectral power densities, this means

$$\Delta S_{\Delta t}(f) = \left(\frac{\varphi_{nl}}{2\pi^2 f T_{rt} v_0} \right)^2 S_I(f) \quad (44)$$

where φ_{nl} is the average value of the peak phase shift and $S_I(f)$ is the power density of the relative intensity noise, and for the timing phase noise

$$\Delta S_{\varphi}(f) = (2\pi f_{rep})^2 \Delta S_{\Delta t}(f) = \left(\frac{f_{rep} \varphi_{nl}}{\pi f T_{rt} v_0} \right)^2 S_I(f). \quad (45)$$

In most cases, at the relaxation oscillation frequency this coupling effect is weak compared to other coupling effects, e.g. the one occurring on a saturable absorber (Sect. 6.1). This holds for the parameters of Fig. 3, when nonlinearity and dispersion for soliton shaping are introduced. However, the nonlinear coupling effect can be important in other cases, such as few-cycle Ti:sapphire lasers, where the nonlinear phase shift is strong while the temporal shift on a saturable absorber is small and the large gain bandwidth leads to negligible Kramers–Krönig effects.

6.4 Raman effect

For femtosecond pulses (particularly for pulse durations < 100 fs), intrapulse Raman scattering [22] tends to cause a red shift of the pulse spectrum for increasing intracavity intensity. Together with the typically anomalous dispersion in such lasers, this results in an increase of the round-trip time [23]. In this way, the Raman effect provides another mechanism for coupling of intensity noise to timing jitter.

6.5 External coupling mechanisms

It is worth mentioning that after leaving the laser cavity the pulses can still experience significant coupling between intensity noise and timing noise. This can be the case when pulses are propagating as solitons in an optical fiber, where the group velocity is dependent on the pulse energy [21] through the self-steepening effect (see Sect. 6.3). Within a long fiber length, such effects can become strong. Also, most techniques for measuring the timing jitter are to some extent sensitive to intensity noise. This applies for measurements based on the radio-frequency spectrum of the photodiode signal [24], particularly in situations where only very few harmonics can be recorded. Even in advanced phase detectors [25], there is some amplitude to timing coupling.

7 Pulse duration noise

The pulse duration is another variable which can exhibit fluctuations. Even if these fluctuations are not relevant by themselves, they must be considered because in some cases they can be coupled to the timing jitter.

Note that even in a soliton mode-locked laser the fluctuations of the pulse duration are not fully correlated with those of the pulse energy, although the average values of pulse duration and energy are inversely related to each other by the action of dispersion and nonlinearity. Starting from the steady state, a fluctuation could well increase the pulse energy without instantaneously shortening the pulse; only the subsequent pulse evolution would affect the pulse duration as well.

Based on these considerations it can be seen that the Haus/Mecozzi model [2], which does not treat the pulse duration as an independent dynamical variable, can not describe fluctuations of the pulse duration. This, however, is not relevant for mode locking with a fast saturable absorber if only the timing jitter is of interest, because in this case the fluctuations of the pulse duration do not affect the timing noise. Also, it makes sense to consider the noise of pulse duration only if the intensity fluctuations are realistically modeled, because for soliton mode-locked lasers these strongly influence the noise in the pulse duration.

For slow saturable absorbers, a coupling from pulse duration noise to timing jitter exists, because the absorber temporally shifts the pulses by an amount which is proportional to the pulse duration (see Sect. 6.1). Note that the pulse duration and pulse energy usually undergo a coupled evolution, and both quantities can affect the timing. To study the effect of pulse duration noise separately, a case can be chosen where the saturation parameter of the absorber is set to ≈ 2.9 , and where the coupling between pulse energy and timing is removed (see Sect. 6.1).

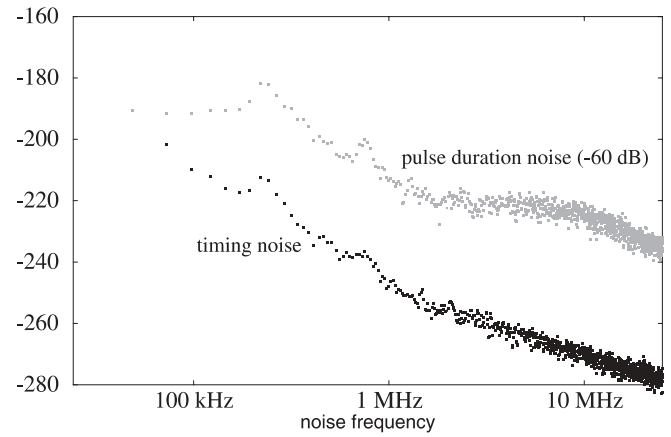


FIGURE 5 Similar to Fig. 4, but with $s = 2.9$ and dispersion and nonlinearity for soliton pulse shaping. The timing phase noise shows a peak at the relaxation oscillation frequency (≈ 0.2 MHz) caused by the relative pulse duration noise (shown with 60 dB subtracted) which is excited by intensity noise and couples to the timing jitter at the slow absorber

As a numerical example, consider a laser as in Fig. 4, but with the saturation parameter $s = 2.9$ and also with dispersion and nonlinearity for soliton pulse shaping. The magnitude of the nonlinearity is chosen so that the peak nonlinear phase shift per round-trip is ≈ 0.1 rad. In addition, the gain bandwidth was increased from 20 nm to 40 nm for better stability of the solitons despite the relatively weak absorber. The results (Fig. 5) show that in the timing noise there is a peak at the relaxation oscillation frequency, caused by pulse duration noise which is excited by intensity noise and couples to the timing jitter at the slow absorber. For comparison, the spectrum of the relative pulse duration noise is also shown. There are also some smaller peaks at higher frequencies in both spectra, the origin of which is not entirely clear. They appear to be related to soliton effects, as their frequencies scale with the strength of dispersion and nonlinearity (but not with various numerical parameters). Note that the frequency corresponding to the soliton period is ≈ 6 MHz, i.e., higher than the observed peak frequencies.

Apart from the direct influence on timing noise, pulse duration noise also couples to intensity noise because for a limited gain bandwidth the effective gain for the pulses depends on the pulse bandwidth. Another coupling effect of this kind occurs at fast absorbers, because fluctuations of the pulse duration affect the peak power and thus the losses at the absorber.

8 Comparison of different types of lasers

8.1 Active versus passive mode locking

When comparing passive mode locking based on fast or slow saturable absorbers, it has been seen that the differences are primarily related to different kinds of coupling of intensity noise (or pulse duration noise) to the timing jitter, while the basic timing noise as derived in Sect. 3 does not depend on details of the absorber.

A fundamental difference, however, exists between active and passive mode locking. With a modulator for active mode locking, there is an external timing reference which provides a restoring force for the pulse timing. Provided that the

noise inputs are not too strong, the timing phase can be stabilized, and its excursions stay limited over arbitrarily long times. Mathematically this means that the timing noise power density does not have a divergence at zero frequency, and the photodiode signal has a spectrum with lines of zero width, despite some noise sidebands. The same holds for a passively mode-locked laser which is timing stabilized using a feedback system. A free-running passively mode-locked laser, however, exhibits timing excursions which grow without bound, mathematically expressed as a divergence of the noise power densities at zero noise frequency and a finite linewidth in the photodiode spectrum [26].

The Haus/Mecozzi model can easily be extended [27] for active mode locking by incorporating the restoring force for the timing. Although this profoundly changes the low-frequency part of the noise spectra, much of the physics of passive mode locking is still valid in this case. Additional noise from the modulator could also easily be included. However, another aspect of active mode locking is that increased timing instabilities occur when the modulation frequency deviates too much from the inverse round-trip time in the laser. It has been shown that these instabilities exhibit features of turbulences in hydrodynamics [9], and the resulting nonlinear dynamics are outside the scope of simple analytical models.

As long as the turbulent regime is avoided in active mode locking, the high-frequency timing noise is similar in both cases. This is due to the fact that this noise is determined not by the mode-locking mechanism but by noise influences from the gain medium.

8.2 Different gain media

Typical mode-locked solid-state lasers, based on bulk crystals or glasses, and typically built with cavity lengths in the order of 1 m, have the potential for extremely low timing jitter because of typically low cavity losses (a few percent), long round-trip times in the nanosecond range, and high powers. However, mechanical vibrations and drifts are difficult to limit for long cavities, so that the low-frequency noise (kHz region and below) can be large, while the high-frequency noise performance can be expected to be very good.

Extremely compact solid-state lasers for multi-GHz repetition rates [4, 5] can easily have lower low-frequency noise due to better mechanical stability, but due to the short cavities they exhibit a higher noise limit from quantum effects. However, the jitter level can be rather low due to the typically low cavity losses (1%–2%).

Mode-locked fiber lasers typically have long cavities, but higher cavity losses and lower powers than solid-state lasers. The mechanical stability can be good if all-fiber solutions are employed (with a fiber-coupled pump diode and no air path within the cavity). With proper overall optimization, a fiber laser can reach or even outperform a bulk solid-state laser in terms of timing jitter, but without this optimization the performance can easily be worse. For multi-GHz pulse repetition rates, harmonic mode locking is usually required, because the cavity length can not be sufficiently reduced for single-pulse operation. This gives the potential for very good noise performance even at high repetition rates, but only when great care is taken to suppress supermode noise [28].

Mode-locked edge-emitting semiconductor lasers typically have very stable, but relatively short cavities, high cavity losses, and low output powers. This sets a high intrinsic noise level due to quantum effects, while additional noise can relatively easily be avoided.

The situation is remarkably different for optically pumped surface-emitting semiconductor lasers with an external cavity (called VECSELs), which can be mode-locked with a SESAM [29]. Here, the noise from the gain medium can be rather low, and the very high output powers [30] minimize the quantum noise contribution to the timing jitter. With a stable cavity, such a laser should exhibit very low timing jitter.

Finally, synchronously pumped parametric oscillators (OPOs) can now be considered. At high noise frequencies, such a device can exhibit a lower timing noise than its pump laser [31], because the pump noise is averaged out over several round-trips if the cavity losses are low. However, even without the influence of pump noise, the parametric gain is associated with parametric fluorescence, in analogy to spontaneous emission in a laser gain medium. It is known that fundamentally the parametric gain contributes the same amount of noise as a four-level laser gain medium. This may be surprising because the overall power loss due to spontaneous emission in a laser gain medium is much higher than the power loss from parametric fluorescence. However, the latter occurs only in the lasing mode, and only this part is relevant for the timing jitter. Another special aspect is related to the issue of imperfect synchronization of OPO and pump laser, which can lead to similar kinds of noise as in detuned actively mode-locked lasers.

9 Conclusions

The issue of noise in mode-locked lasers, and in particular of timing jitter in passively mode-locked lasers, has been addressed in detail using a combination of analytical and numerical methods. The results of the analytical Haus/Mecozzi model are very useful even for a much broader class of lasers than originally anticipated, because the key results can be derived without referring to soliton perturbation theory, so that the associated restricting assumptions are no longer required. On the other hand, it has been seen that other cases involve additional effects which would be difficult to cover with extensions of the Haus/Mecozzi model. The basic limitations are the gain saturation model, which is unrealistic for solid-state lasers, and the small number of dynamical variables, which excludes the treatment of additional effects of interest, as the fluctuations of the pulse duration. In particular, various important effects occur for lasers mode-locked with slow saturable absorbers, as SESAMs [18].

The discussion of quantum noise effects associated with the laser gain and the cavity losses has been the main focus. Particularly in free-running passively mode-locked lasers, where there is no restoring force for the pulse timing, these quantum effects cause the generated pulse trains to exhibit a timing noise which at low noise frequencies is orders of magnitude stronger than the quantum-limited timing noise as clarified in Sect. 2. Additional low-frequency noise is introduced particularly by pump fluctuations exciting intensity noise, which can couple to the timing noise through various

mechanisms, some of which have been discussed in depth in Sect. 6. Note that such an influence on the timing noise can occur even for a shot-noise-limited pump source, as it is known that a significant part of the intensity noise around the relaxation oscillation frequency is caused by unavoidable quantum noise [12].

Note also that even for a hypothetical noiseless gain medium (without pump noise and spontaneous emission) there would still be the quantum noise introduced by the cavity losses, which is similar in strength to the noise from a four-level laser gain medium. Therefore, the only way to significantly decrease the quantum-limited timing jitter is to decrease the cavity losses (and accordingly the amount of required gain), and to increase the round-trip time T_{rt} , because the quantum noise input per second is governed by gain and loss experienced in one second. The dependence on the round-trip time also applies to other noise effects, those of vibrating cavity mirrors. Here, the timing noise power even scales with T_{rt}^{-2} . On the other hand, for technical reasons the mechanical vibrations of the cavity length tend to be larger for long cavities. This effect together with the difficulty of measuring very weak timing noise is the reason why quantum-limited timing jitter performance [11, 27, 32, 33] is more easily seen for compact laser cavities with relatively high losses, where quantum noise influences are relatively strong while classical noise inputs can be effectively minimized.

It has been pointed out [34] that for a given pulse repetition rate one can achieve a lower timing jitter by harmonic mode locking, i.e., by using a longer laser cavity with multiple equally spaced circulating pulses. This result becomes obvious through the discussion above. However, harmonic mode locking is not only affected by the greater difficulty of making a longer cavity mechanically stable, but is also plagued by supermode noise [34], which can strongly increase the noise powers near harmonics of the pulse repetition frequency. Therefore, harmonically mode-locked lasers need special efforts [28] to realize the theoretical potential for very low timing noise over a wide frequency span.

Another interesting remark concerns the fact that many noise effects in a laser cavity are most naturally described as affecting the round-trip time (via the cavity length) and not directly affecting the temporal positions of pulses. This has important implications for the noise spectra. The timing errors result from changes of the round-trip time by a temporal integration, so that the timing noise power then scales with f^{-2} times the power density of the original noise input. For example, most of the effects discussed in Sect. 6, which couple intensity noise to timing jitter, have this property. The coupling strength scales with f^{-2} , so that the coupling becomes most important at low noise frequencies. For this reason, in free-running passively mode-locked lasers the frequency dependence of timing noise can become very strong at low frequencies.

In this context it is important to note that the effects of drifts (e.g. of the cavity length) or flicker noise (e.g. in the pump source) have not been explicitly discussed. Such noise sources are frequently encountered in reality and tend to particularly affect the low-frequency noise. One can take

them into account by translating $1/f$ pump noise into timing noise using the analytically calculated coupling factors from Sect. 6.

ACKNOWLEDGEMENTS The author is grateful to Ursula Keller for stimulating this work and thanks Harald Telle for various useful discussions and comments on the manuscript.

REFERENCES

- 1 R. Paschotta: Appl. Phys. B DOI 10.1007/s00340-004-1547-x (2004)
- 2 H.A. Haus, A. Mecozzi: IEEE J. Quant. Elect. **QE-29**, 983 (1993)
- 3 L.A. Jiang, M.E. Grein, H.A. Haus, E.P. Ippen: IEEE J. Sel. Top. Quant. Elect. **7**, 159 (2001)
- 4 L. Krainer, R. Paschotta, S. Lecomte, M. Moser, K.J. Weingarten, U. Keller: IEEE J. Quant. Elect. **QE-38**, 1331 (2002)
- 5 L. Krainer, R. Paschotta, G.J. Spühler, I. Klimov, C.Y. Teisset, K.J. Weingarten, U. Keller: Electron. Lett. **38**, 225 (2002)
- 6 T.R. Schibli, J. Kim, O. Kuzucu, J.T. Gopinath, S.N. Tandon, G.S. Petrich, L.A. Kolodziejski, J.G. Fujimoto, E.P. Ippen, F.X. Kärtner: Opt. Lett. **28**, 947 (2003)
- 7 H.A. Haus, M. Margalit, C.X. Yu: J. Opt. Soc. Am. B **17**, 1240 (2000)
- 8 A.M. Braun, V.B. Khalfin, M.H. Kwakernaak, W.F. Reichert, L.A. Di-Marco, Z.A. Shellenbarger, C.M. DePriest, T. Yilmaz, P.J. Delfyett, J.H. Abeles: IEEE Photon. Technol. Lett. **14**, 1058 (2002)
- 9 F.X. Kärtner, D.M. Zumbühl, N. Matuschek: Phys. Rev. Lett. **82**, 4428 (1999)
- 10 H.A. Haus, A. Mecozzi: IEEE J. Quant. Elect. **QE-30**, 1966 (1994)
- 11 L.A. Jiang, M.E. Grein, E.P. Ippen, C. McNeilage, J. Searls, H. Yokoyama: Opt. Lett. **27**, 49 (2002)
- 12 C.C. Harb, T.C. Ralph, E.H. Huntington, D.E. McClelland, H.-A. Bachor: J. Opt. Soc. Am. B **14**, 2936 (1997)
- 13 F.X. Kärtner, L.R. Brovelli, D. Kopf, M. Kamp, I. Calasso, U. Keller: Optical Engineering **34**, 2024 (1995)
- 14 C. Hönninger, R. Paschotta, F. Morier-Genoud, M. Moser, U. Keller: J. Opt. Soc. Am. B **16**, 46 (1999)
- 15 A. Schlatter, S.C. Zeller, R. Grange, R. Paschotta, U. Keller: to appear in J. Opt. Soc. Am. B (2004)
- 16 R. Paschotta, U. Keller: Appl. Phys. B **73**, 653 (2001)
- 17 U. Keller, D.A.B. Miller, G.D. Boyd, T.H. Chiu, J.F. Ferguson, M.T. Asom: Opt. Lett. **17**, 505 (1992)
- 18 U. Keller, K.J. Weingarten, F.X. Kärtner, D. Kopf, B. Braun, I.D. Jung, R. Fluck, C. Hönninger, N. Matuschek, J. Aus der Au: IEEE J. Sel. Top. Quant. Elect. **2**, 435 (1996)
- 19 C.H. Henry: IEEE J. Quant. Elect. **QE-18**, 259 (1982)
- 20 G.P. Agrawal: Nonlinear Fiber Optics (Academic Press, San Diego, CA, 1989)
- 21 H.A. Haus, E.P. Ippen: Opt. Lett. **26**, 1654 (2001)
- 22 G.P. Agrawal: Nonlinear Fiber Optics (Academic Press, San Diego, CA, 2001)
- 23 N. Haverkamp, H. Hundertmark, C. Fallnich, H.R. Telle: Appl. Phys. B **78**, 321 (2004)
- 24 D. v. d. Linde: Appl. Phys. B **39**, 201 (1986)
- 25 R.P. Scott, C. Langrock, B.H. Kolner: IEEE J. Sel. Top. Quant. Elect. **7**, 641 (2001)
- 26 D. Eliyahu, R.A. Salvatore, A. Yariv: J. Opt. Soc. Am. B **14**, 167 (1997)
- 27 M.E. Grein, L.A. Jiang, H.A. Haus, E.P. Ippen, C. McNeilage, J.H. Searls, R.S. Windeler: Opt. Lett. **27**, 957 (2002)
- 28 C.M. DePriest, T. Yilmaz, P.J. Delfyett, S. Etemad, A. Braun, J. Abeles: Opt. Lett. **27**, 719 (2002)
- 29 S. Hoogland, S. Dhanjal, A.C. Tropper, S.J. Roberts, R. Häring, R. Paschotta, U. Keller: IEEE Photon. Technol. Lett. **12**, 1135 (2000)
- 30 R. Häring, R. Paschotta, A. Aschwanden, E. Gini, F. Morier-Genoud, U. Keller: IEEE J. Quant. Elect. **QE-38**, 1268 (2002)
- 31 J.M. Dudley, D.T. Reid, M. Ebrahimzadeh, W. Sibbett: Opt. Commun. **104**, 419 (1994)
- 32 D.E. Spence, J.M. Dudley, K. Lamb, W.E. Sleat, W. Sibbet: Opt. Lett. **19**, 481 (1994)
- 33 S. Namiki, C.X. Yu, H.A. Haus: J. Opt. Soc. Am. B **13**, 2817 (1996)
- 34 T. Yilmaz, C.M. DePriest, A. Braun, J.H. Abeles, P.J. Delfyett: IEEE J. Quant. Elect. **QE-39**, 838 (2003)